

Figure 7.1. Schematic phase diagram of noncrystalline water. Liquid water is stable above the melting temperature line $T_M(P)$. Below this temperature and above the homogeneous nucleation temperature $T_H(P)$ liquid water is metastable (supercooled). The “no man’s land” is the region where crystallization cannot be avoided experimentally. Glassy water exists below the crystallization temperature $T_X(P)$. $T_g(P)$ is the glass transition temperature above which glassy water becomes an ultraviscous liquid. For glassy water at 1 bar, $T_g \sim 136\text{K}$; it is not clear yet what the value of $T_g(P)$ is at high pressures (horizontal dashed line). Two different glassy forms are identified at $P < 0.325$ GPa, LDA and HDA. The solid line separating the LDA and HDA regions extends into the “no man’s land” (dashed line); see also Figure 8b. Adapted from Ref. [5].



Figure 7.7. Amorphous ice sample (1.5 mL) made by decompression of VHDA (see Section VII) at 140K to 0.07 GPa with a rate of 13 MPa min^{-1} and then quench-recovered to 77K and 1 bar (top image). After removal from the piston cylinder apparatus, the sample easily broke into two pieces; the two separated pieces were placed on a copper block kept at 77K (second from top). The bottom two images show the two pieces in the course of heating to 250K at 1 bar. Adapted from Ref. [68].

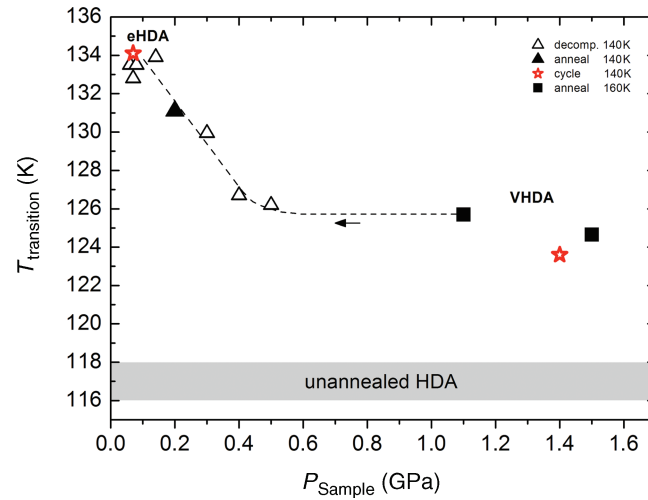


Figure 7.9. Thermal stability of various amorphous ices at ambient pressure. Samples were quench-recovered at 77K and 1 bar, and heated at a rate of 10K min^{-1} using a differential scanning calorimeter. $T_{\text{transition}}$ is the onset temperature at which the samples transform to LDA. Closed squares: VHDA samples (Section VII) obtained by isobaric heating uHDA at high pressure ($P_{\text{sample}} = 1.1$ and 1.5 GPa) to 160K. Open triangles: HDA samples obtained by decompression of VHDA at 140K to $P = P_{\text{sample}}$ and then quench-recovered from the selected pressure. Closed triangle: HDA sample heated to 140K at 0.2 GPa. Stars: decompression cycle between eHDA and VHDA at 140K (see Figure 10). Unannealed HDA is prepared at 77K by pressure-induced amorphization of ice I_h (see Section II). The data are taken from Refs [21,68]. Symbol sizes represent error bars of $\pm 0.5\text{K}$.

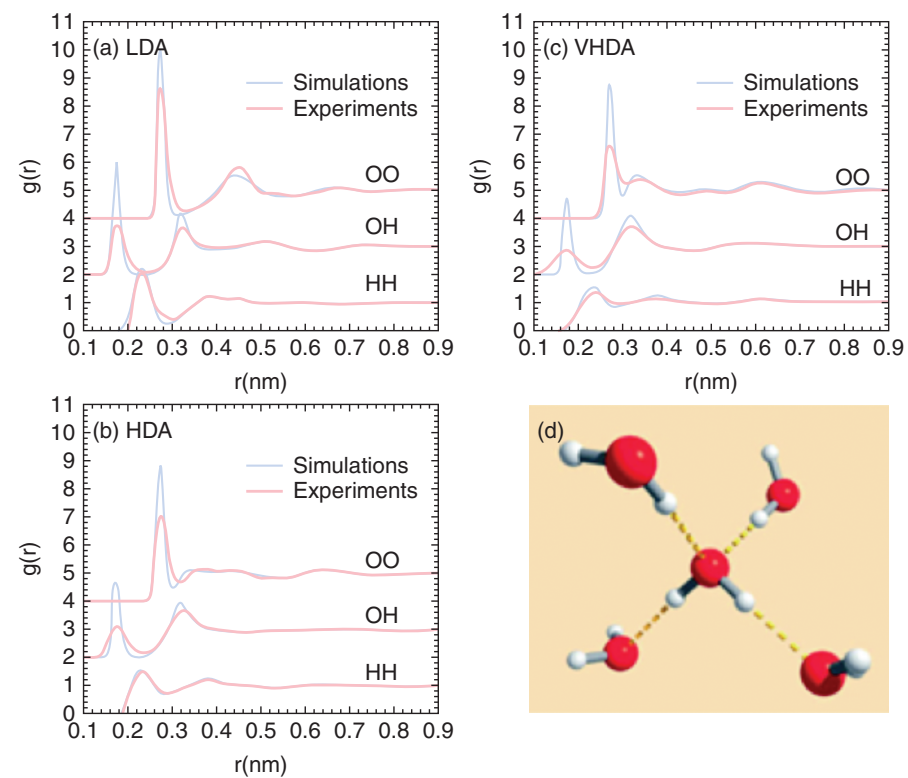


Figure 7.12. Radial distribution functions of (a) LDA, (b) HDA, and (c) VHDA as compared between simulations [87] and experiments [56,85]. (d) The Walrafen pentamer is the basic structural motif common to all amorphous ices. Adapted from Ref. [7].

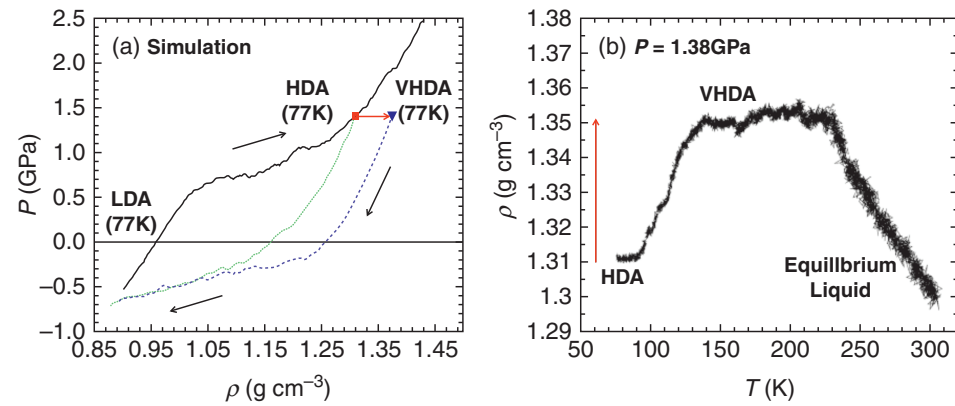


Figure 7.13. (a) Pressure versus density during the (i) LDA-to-HDA transition (solid line), (ii) decompression of HDA at $T = 77\text{K}$ (dotted line), and (iii) decompression of VHDA at $T = 77\text{K}$ (dashed line). The gray arrow indicates the density change in HDA upon isobaric heating at $P = 1.38$ GPa from $T = 77\text{K}$ (square) to 165K , followed by cooling back to $T = 77\text{K}$ (triangle). (b) Evolution of density upon annealing HDA at $P = 1.38$ GPa. From Ref. [87].

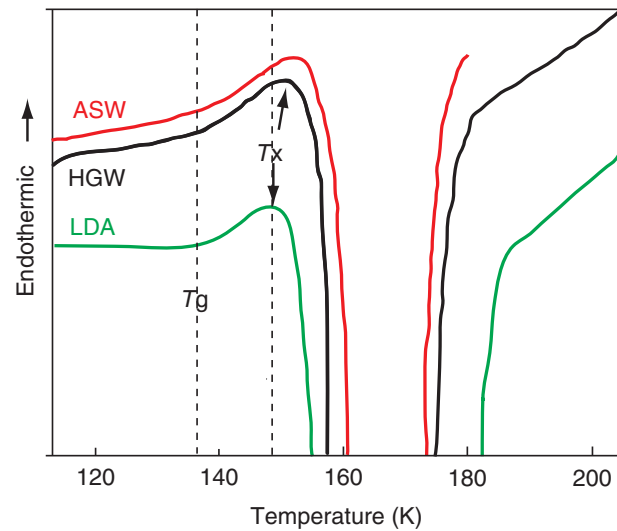


Figure 7.14. DSC scans of ASW, HGW, and LDA at 1 bar. All traces are recorded at 30K min^{-1} after prior annealing at 127–130K for at least 90 min. Vertical dashed lines mark the glass transition temperature $T_g \approx 136\text{K}$, for all three samples, and the crystallization temperature $T_x \approx 148\text{K}$, for the case of LDA. In between these vertical lines the sample is in an ultraviscous, deeply supercooled liquid state. Adapted from Refs [101–103].